9

A Rational Design Approach for Developing Immunomodulators Based on CD4 and CD8

ANNA P. TRETIAKOVA, ROSS H. ALBERT AND BRADFORD A. JAMESON*

Department of Biochemistry, School of Medicine, MCP Hahnemann University, 245 North 15th Street, Philadelphia, PA 19102, USA

Introduction

The pharmaceutical industry has classically relied on screening methods for its discovery and development of new drugs. Moreover, the recent use of high throughput screening has radically changed the industry's ability to expand drug searches. These approaches have proven to be highly successful and account for > 90% of all of the prescription drug market. From a 'Company' perspective, the more compounds screened, the greater the likelihood that a new drug can be added to the 'pipeline'. Although random screens are time-consuming and labour-intensive, these methods have a proven success record and are unlikely to change in the near future. Today, the compound libraries are, generally, the products of shotgun combinatorial chemistry or are collections of natural products. The screens, by necessity, are designed for 'ease-of-use'. Consequently, the initial system must have a simplified read-out for screening potential drug 'hits'. Often, this means that the assay read-out has been reduced to monitoring the formation or disassociation of a protein complex or for monitoring the expression of an engineered marker, such as luciferase, to screen for

*To whom correspondence may be addressed (bjameson@drexel.edu)

Abbreviations: CD4, cluster designation 4; CD8, cluster designation 8; FDA, Food and Drug Administration; HIV, human immunodeficiency virus; AIDS, acquired immune deficiency syndrome; gp, glycoprotein; MS, multiple sclerosis; TCR, T cell antigen receptor; MHC II, major histocompatibility complex class II; APCs, antigen-presenting cells; CDRs, complimentarity determining regions; NMR, nuclear magnetic resonance; MLR, mixed lymphocyte reaction; EAE, experimental allergic encephalomyelitis; GVHD, graft versus host disease; MassSpec, mass spectrometry; HPLC, high pressure liquid chromatography; 2D NMR, 2-dimensional NMR; SAR, structure–activity relationship; MuLV, murine leukaemia virus; CTL, cytotoxic T lymphocyte; mAb, monoclonal antibody; FACS, fluorescence-activated cell sorting; NP, nuclear protein; NPP, NP peptide; IL-2, interleukin 2; IL-2R, IL-2 receptor; AICD, activation-induced cell death; D1D2, domain1 domain2; FFU, focus forming units; FITC, fluorescein isothiocyanate; Cy5PE, cyanine5 phycoerythrin; PE, phycoerythrin; i.p., intraperitoneal; i.v., intravenous; CPM, counts per minute; Fmoc, 9-fluorenylmethoxycarbonyl.

Biotechnology and Genetic Engineering Reviews – Vol. 19, November 2002
0264–8725/02/19/175–203 $20.00 + $0.00 © Intercept Ltd, PO Box 716, Andover, Hampshire SP10 1YG, UK

perturbations within a signal transduction pathway. All positive hits within the system need to be further evaluated for biological activity to ferret out the false positive and potentially toxic compounds. Any compound designated as a true 'hit' must be turned over to a team of medicinal chemists in order to deduce the minimal elements responsible for the observed biological activity. This pharmacophore is then used as a 'lead' compound to develop a potential drug. In this way, modern screening methods allow researchers to identify effective drugs without actually understanding the mechanism of its action. In many cases, this leads to the development of a drug with unanticipated side effects and toxicities.

In general, it is understood that the use of a rational design strategy for engineering lead compounds would dramatically reduce both the time and cost of bringing a drug to market. The problem, however, becomes one of risk versus benefit. Without explicit rules and protocols that describe *how* to design a drug, structure-based engineering of a potential drug represents a large risk to a conservative company. It is clearly better to have a drug in-hand than it is to have a series of potential drugs '*in silico*'. As long as there is a perceived likelihood that random screening presents the greatest chance of success for developing a new drug, even though it is a more cost-intensive approach, it will be the approach 'of choice'. The cost of discovery and development of any drug is built into its market pricing policies. Thus, the cost is justified. Although the development of rational drug design strategies will clearly have a dramatic impact on the future of the pharmaceutical industry, a body of fundamental principles must be established before its use can be widely implemented. Consistent with the needs of the industry, the rational design process is now being implemented in a slow and conservative fashion.

Whether or not the drug discovery process is mediated by random screening or by a premeditated design approach, the general process requires a validated target. The target can be a pathway or a single component of the pathway that has been proven to be a part of a rate-limiting process in the establishment/maintenance of a human disease. Perturbation of this target, through drug intervention, should have a beneficial therapeutic effect. In terms of rational drug design, the targets have been almost exclusively enzymes. The design of active site inhibitors has been an ideal entry point for pharmaceutical companies into the rational drug design arena. With an enzyme of known three-dimensional structure, the geometry and the physical placement of the hydrogen bond donors/acceptors is clearly delineated. Thus, the drug design groups have access to a validated target with a well-defined structural template, i.e. the active site. The inhibitor design process then becomes an exercise of creating an organic molecule that matches the Van der Waals surface of the active site and presents donor/acceptor groups in the appropriate orientations. Although this is definitely not a trivial exercise, the likelihood of designing a successful drug is high.

There are now several examples of FDA-approved drugs that have come to market as a result of structure-based design strategies. The design and development of inhibitors of the HIV protease as a therapeutic treatment for AIDS patients is, perhaps, the most illustrative example of the attention industry has paid to the rational design process. The HIV-encoded protease is known to provide a rate-limiting step in the life cycle of the virus and is, therefore, a good therapeutic target. The first accurate structure of the protease was published in 1989 (Wlodawer *et al.*). Within a year and a half of this report, there were a variety of pharmaceutical companies already

publishing reports of rationally designed inhibitors (Erickson *et al.*, 1990 [Abbott Laboratories]; Craig *et al.*, 1991 [Roche]; DeSolms *et al.*, 1991 [Merck, Sharp & Dohme]; Reddy *et al.*, 1991 [Agouron Pharmaceuticals, Inc.]; Thaisrivongs *et al.*, 1991 [Upjohn Company]). These rationally designed drugs, in combinations with reverse transcriptase inhibiting nucleoside analogues in 'triple drug cocktails', have dramatically improved the life span of HIV-infected people (Matsushita, 2000).

In order to ensure a reasonable chance of designing a new drug, there must pre-exist a reasonable template from which the drug will be engineered. Enzymes offer an active site, but the problem becomes considerably more complicated when addressing the design of drugs intended to perturb protein–protein interactions. Relative to an active site, the surface engaged in contacting another protein is large. *A priori*, there is no 'road map' for describing which part of the contact surface should be used as a design template. In fact, until recently, it was thought that a small molecule could not be used to compete with a high affinity protein–protein interaction because of the overwhelming number of contact points on the proteins relative to the small size of the drug. One of the events that helped to change this perception was the development of small organic molecules that block the binding of the fibrinogen receptor, gpIIa/IIIb, to fibrin on platelets. In 1984, Pierschbacher and Ruoslahti (1984) published a paper in *Nature* describing a small tetrapeptide sequence, R-G-D-S, which constituted a common recognition element in the binding of integrins to their receptors. It was later discovered that the core sequence of the tetrapeptide, R-G-D, helped mediate the binding between fibrin and gpIIb/IIIa (Brown and Goodwin, 1988). Rational design groups at several large pharmaceutical companies were able to turn the low affinity, promiscuous R-G-D peptide into a high affinity, high specificity organic drug that is in current clinical use [Tirofiban (Merck Research Laboratories; Hartman *et al.*, 1992) and Lamifiban (F. Hoffman-La Roche Ltd; Carteaux *et al.*, 1993)]. The success of this effort underscores the willingness of the pharmaceutical industry to engage in a structure-based design effort, if a design template, such as the R-G-D motif, can be clearly identified on a validated target. Furthermore, this work points to the feasibility of designing small analogues to block protein–protein binding interactions. In this vein, our laboratory, over the last 10 years, has focused its efforts on the identification of protein–protein binding surfaces and on the delineation of small surface areas that constitute drug design templates. All of our work has involved the design of small molecule/peptide-based modulators of the immune system. In this review, we will describe two different protein systems that were used to delineate drug design templates on the CD4 protein (targetted to develop modulators of helper T cells) and the CD8 protein (targetted to develop modulators of cytotoxic T cell responses).

Targetting the CD4 protein–protein interactions on helper T cells

Multiple sclerosis (MS) is a relapsing/remitting autoimmune disease of the central nervous system. It is characterized by inflammatory cell damage of the myelin sheath, resulting in a slowing or blockage of nervous transmission. Currently, the most effective approved treatments for MS patients are the use of genetically engineered beta-interferon or a mixed synthetic co-polymer, both of which serve, statistically, to reduce the number of newly formed plaques during an MS attack (Lucchinetti *et al.*, 2001; Rolak, 2001). This treatment is expensive, requires a direct injection of the

protein, and is not always very effective. There is a clear need for improved therapeutic strategies.

Although the etiology of the disease is unknown, CD4-positive helper T cells appear to be crucial mediators of both disease onset and progression (Hutchings *et al.*, 1993). Consequently, there has been a major effort in many different laboratories to target the activated subset of helper T cells, responsible for the inflammatory damage, as a means of improving the existing therapies for MS patients.

The CD4-positive helper T cells are predominantly produced in the thymus, where they undergo both positive and negative selection. Each helper T cell produced in this organ is unique by virtue of its polymorphic T cell antigen receptor (TCR) that is matched to the resident major histocompatibility complex class II (MHC II) proteins. The mature cells that emerge are highly diverse and are selected as discriminators of self versus non-self. As these cells migrate to the periphery, they become responsive to peptide antigens presented within the groove of the MHC II heterodimer on antigen-presenting cells (APCs) (Brown *et al.*, 1993). Under normal circumstances, only the helper T cells bearing a TCR that appropriately fits to the foreign antigen-bearing APC will become activated. The rest of the subset of CD4-positive cells remains quiescent. The activated T cell clonally proliferates, secreting growth factors and cytokines, and aids in the mounting of both humoral as well as cytotoxic immune responses.

In autoimmune conditions, such as multiple sclerosis or Crohn's disease, an aberrant constellation of events occur, such that a clonal activation of a CD4-dependent T cell is set in motion to create a pathologic inflammatory response. The key to treating the symptoms associated with these disease states is to target the activated set of helper T cells. In an otherwise healthy autoimmune patient, the only activated T cells are those involved in the pathogenic responses; the rest of the repertoire is resting.

The objective of our drug design efforts is to identify surface regions on CD4 that can be used to engineer 'lead compounds' that can be used in the treatment of autoimmune diseases and in the treatment of the rejection symptoms associated with transplantation. The strategic intent is to design compounds that can disrupt the primary activation signal (generated through the T cell activation cluster) in the helper T cells, thus inducing programmed cell death/anergy in the activated cell. The analogues are designed to induce clonal deletion (or anergy) only in the activated sets of T cells without affecting the resting repertoire of cells needed to mount new responses. Thus, if one can design an appropriate mimetic of the CD4 surface, it can be used to perturb the primary signal transduction pathway in activated helper T cells. This should result in the functional deletion of these cells and create a hole in the immunologic repertoire, preventing the reoccurrence of the targetted activation response.

The CD4 is a member of the immunoglobulin superfamily of proteins. The first two amino terminal domains of the human CD4, which are thought to confer the major contacts for driving the primary T cell activation pathway forward, were crystallized (Ryu *et al.*, 1990). In order to validate any of our synthetic constructs in an *in vivo* model of CD4-dependent responses, we opted to use a murine system. Because the hydrophobic core is well conserved between the human and murine CD4 (the principal differences occur as a result of surface decoration), we created an homology model of the murine CD4 (for a review of the approach used in the homology

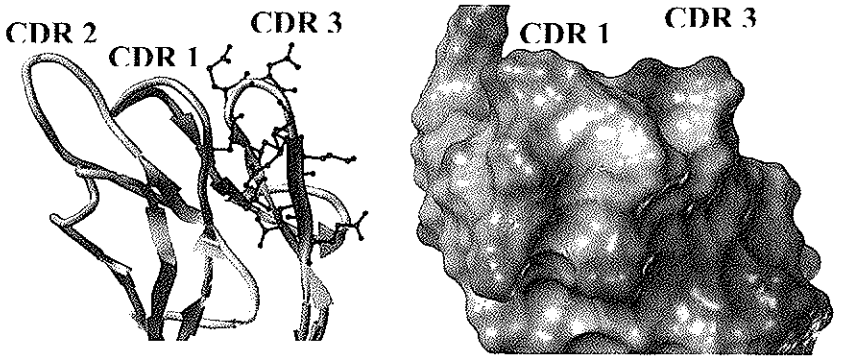

Figure 9.1. Molecular model of the murine CD4. Part of the solvent exposed CD4 surface is formed by the juxtaposition of the CDR-like regions 1, 2 and 3. The left panel shows the basic fold of the CDR-like regions in the tube-ribbon representation. Ball-and-stick rendering shows positions of the individual side chains, which comprise the CDR3-like region. The right panel is the Connolly surface formed by the CDR-like regions. The homology model of the extracellular domains (D1D2) of the murine CD4 protein was built based on human CD4 structure (PDB accession number is 1CDH) as described in Jameson (1989) and McDonnell *et al.* (1992a,b).

modelling, see Jameson, 1989). We used the murine CD4 as a starting structure for the studies described below (see *Figure 9.1*). Structurally, the first amino terminal domain of CD4 is closely related to an antibody's light chain variable domain. An antibody possesses unique (hypervariable) domains, known as complementarity-determining regions (CDRs), which comprise the antigen-binding surface of the antibody. This surface is formed by the juxtaposition of the CDR1, CDR2 and CDR3 domains. Although CD4 does not have hypervariable domains, it possesses regions that are structurally analogous to the CDRs (*Figure 9.1*). In our initial attempts to define a surface region on the CD4 surface that could serve as a potential drug design template, we focused our efforts on these CDR-like regions. Of the 3 CDRs, only analogues of the CDR3-like domain were able to inhibit CD4-dependent T cell responses (McDonnell *et al.*, 1992a). The active analogues of the CDR3-like region of the murine CD4 were derived from the native sequence Cys-Glu-Val-Glu-Asn-Arg-Lys-Glu-Glu (see *Figure 9.2*), and were designed to mimic the surface presented by the native protein. The design strategy employed the artificial introduction of a disulphide bridge to appropriately restrain the conformation of the peptide. Nuclear magnetic resonance (NMR) studies indicated that the biologically active surface could be presented by the insertion of a 'forced turn' using a proline–glycine–proline (PGP) motif (McDonnell *et al.*, 1992b). The side chain of a proline residue forms a pyrrolidine ring that is covalently bonded to the backbone nitrogen atom of the peptide group. This limits the rotation about the N-alpha:C-alpha (phi) bond of the backbone, with the adjacent C-alpha:C (psi) bond restricted to bond angles of about −55° and +130° (Degrado, 1988). In contrast, the inherent flexibility of the glycine residue allows for the occurrence of the tight turn, strongly induced by the rigid neighbouring prolines, without the steric side chain constraints other amino acids would experience. Energy-dependent simulations of molecular motion (molecular

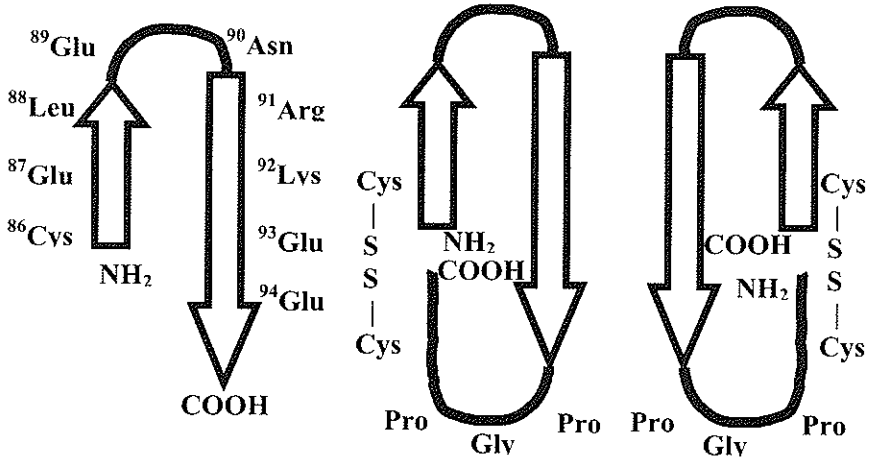

Figure 9.2. Schematic diagram of the designed mPGPtide. The left panel shows the orientation and the native amino acid sequence (with the corresponding amino acid numbers) of the murine CDR3-like region of the CD4 protein. The middle and the right panels show the schematic diagrams of the conformationally restrained mPGPtide and the retro-inverso mPGPtide, respectively. The arrows represent the beta strands within the CDR3-like region. The positions of the artificial disulphide bonds along with the amino- and carboxy-termini are indicated. Note the inverted backbone orientation on the right panel.

dynamics calculations) of the CDR3 analogue containing the PGP motif, in conjunction with random searches of conformational space, led to a family of stable structures displaying a surface similar to that of the murine CD4 model. NMR analysis was used to confirm the modelling predictions (McDonnell *et al.*, 1992b).

In order to validate the designed CD4 mimetics, we needed to show their ability to dose-dependently inhibit an *in vitro* CD4-dependent response, as well as to inhibit the CD4-dependent response, *in vivo*, in an intact animal (Jameson *et al.*, 1994). Considering the relatively large size of the analogue, 13 amino acids, it seemed likely that it would be rapidly degraded *in vivo*. To protect against this type of proteolysis, we opted to employ the use of 'D' enantiomeric amino acids instead of the naturally occurring 'L' form. It has been shown that one can re-create the original L-amino acid side chain surface presentation with D-amino acids, if one reverses the sequence order [where the amino terminal end of the peptide becomes the carboxy terminal end] (Chorev *et al.*, 1979). This type of peptide design has become known as a 'retro-inverso' construct. For our initial *in vitro* assays, we constructed two control analogues. The first was a 'PGP' construct of the CDR3-like domain from the human CD4. Because there is not much cross-reactivity between the murine CD4 and human CD4 proteins, we synthesized a human analogue that had similar conformational features to the equivalent murine analogue but possessed a different surface decoration. The second control was to synthesize a version of the retro-inverso murine 'PGP' analogue with the same amino acid composition but a randomized sequence order, i.e. a scrambled version of the murine [retro-inverso] PGPtide. The primary screen used to assess biological activity was a murine mixed lymphocyte reaction (MLR). This is an assay using active primary lymphocytes from an inbred mouse strain to respond to an allogeneic stimulus (in a CD4-dependent fashion). Fixed macrophages from a

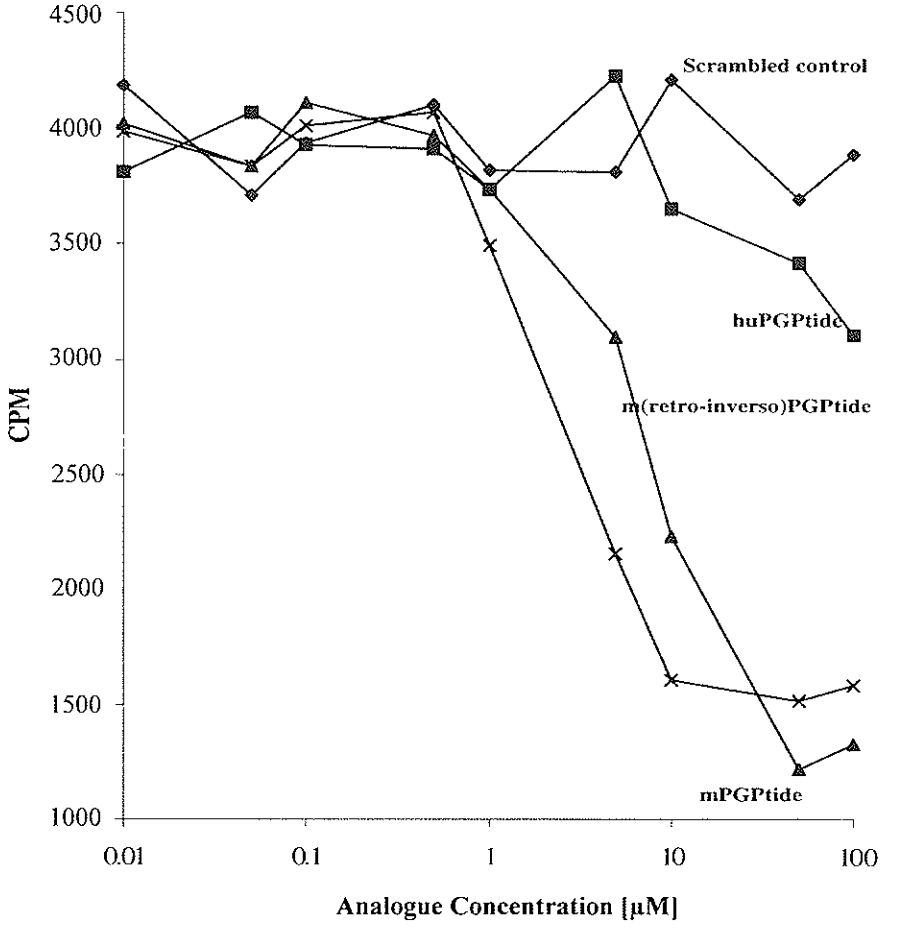

Figure 9.3. Titration of the designed and control analogues in the murine MLR. The names of the analogues used in this assay are indicated next to the respective lines on the graph. The analogues were used at 100, 50, 10, 5, 1, 0.5, 0.1, 0.005, and 0 micromolar concentrations. The MLR was performed as described in Jameson *et al.* (1994).

genetically disparate inbred mouse provide the initiating stimuli. ^{3}H-Thymidine is added to the culture prior to harvest in order to label newly synthesized DNA. Typical results from the murine MLR are shown in *Figure 9.3*. The conformationally restrained mPGP and its retro-inverso construct both exhibited dose-dependent inhibition of the MLR, whereas the control analogues were inactive. The success of a designed analogue *in vitro*, however, does not signify that it will have a similar efficacy profile *in vivo*.

Initially, the retro-inverso mPGPtide was tested for efficacy in a murine model of human multiple sclerosis, experimental allergic encephalomyelitis [EAE]. In EAE, an autoimmune inflammatory response is forced against the animal's myelin sheath, resulting in symptoms similar to what one observes in the human disease. Using this model, we were able to show that the designed analogue was able to inhibit both the clinical incidence and severity of EAE with a single injection, but without depleting

the CD4+ subset and without the inherent immunogenicity of an antibody (Jameson *et al.*, 1994; Marini *et al.*, 1996). This analogue was also able to exert its effects on disease even after the onset of symptoms. Moreover, untreated (or control-treated) mice exhibited moderately severe inflammation with extensive perivascular cuffing throughout the CNS tissue. In contrast, the mice treated with the retro-inverso mPGPtide exhibited very mild meningeal mononuclear cell infiltration, with only a few detectable perivascular cuffs in the spinal cord (Marini *et al.*, 1996).

The retro-inverso analogue was further tested in several other CD4-dependent animal models. One of these animal models exploits graft-versus-host disease (GVHD) similar to that observed in bone marrow patients. GVHD represents a formidable challenge to transplantation clinicians. The designed CD4 analogue was able to significantly reduce, and in some cases ablate, the CD4-dependent GVHD in rodent bone marrow transplants (Townsend *et al.*, 1996; Koch and Korngold, 1997; Townsend *et al.*, 1998). Allogeneic skin grafting is another animal model that has been used. Because of the highly vascular nature of these tissues, inhibiting skin graft rejection has proven to be extraordinarily difficult. The retro-inverso analogue can significantly prolong graft survival in an MHC class II mismatched skin graft and works synergistically in combination with cyclosporin A (Koch *et al.*, 1998). Finally, this analogue has been shown to significantly reduce mortality in a murine model of ulcerative colitis under circumstances where the CD4 monoclonal antibody has only a marginal effect (see *Table 9.1*) (Okamoto *et al.*, 1999).

The diverse set of animal models all indicated that the *in vivo* activities parallel the observed *in vitro* activities. A single bolus injection of the designed analogue appears to exert its effect only on the activated set of CD4+ T cells without any residual effects on the resting cell populations. Although the potency of the designed CD4 mimetic is too low to qualify as a drug candidate (the IC_{50} is in the low to mid micromolar range), the biological data suggested that this analogue could have been an interesting 'lead' molecule. The insurmountable obstacle for the retro-inverso CD4 analogue's potential success as a lead molecule was its batch-to-batch variations in biological activity. It was observed that the final product, although chemically pure (purity was judged via MassSpec, capillary electrophoresis and reverse phase HPLC), did not always have the same biological activity as the previously synthesized batch. There were clearly 'good' and 'bad' batches. Presumably, the observed variability in the biological activity of the different batches of the analogue was not due to the synthetic procedures, rather due to variations in the refolding process that determine the final presented conformations of the peptide. The assumption was that multiple conformational populations of peptide are present in all batches of the synthesized product. The dominant conformation determined the level of observed biological activity. To address this hypothesis, we analysed a chemically pure batch of the mPGP, giving a single clean peak upon analytical HPLC. The purified peptide was loaded onto a preparative HPLC column and the single peak was collected into three pools as it came off the column. Fraction I appeared to retain most of the biological inhibitory activity. In collaboration with Dr Markus Germann (Thomas Jefferson University, Philadelphia, PA, USA), the three fractions (I, II and III) were analysed by high resolution NMR (600 MHz Bruker AMX Spectrometer). All three fractions had identical molecular masses. The NMR analysis revealed significant differences in the three fractions (unpublished observations). It was apparent that fraction II was a

Table 9.1. Effect of various treatment modalities on the outcome of TNB-induced colitis in mice (for experimental details, see Okamoto *et al.*, 1999).

Treatment	Mortality (%)	Average grade of inflammation
None	57.2 (8/14)	2.33
Retro-inverso mPGPtide (scrambled control)	50.0 (2/4)	2.5
Isotype IgG control	60 (3/5)	2.0
Retro-inverso mPGPtide	16.7 (1/6)	0.33
Anti-CD4 mAb	50 (3/6)	1.33

mixture of fraction I and fraction III. The most obvious difference was a multiplet structure of glycine in the PGP constructs for fraction I, while in fraction III this multiplet was collapsed. These data indicated that there were different structures for each of the fractions. Furthermore, there was no evidence of inter-conversion of the structures from fraction I and fraction III (or if so, their conversion was very slow). If the constraining disulphide bond was reduced with deutro-β-mercaptoethanol, all of the fractions showed virtually identical NMR spectra. Thus, it appeared that the different and locked conformations are a direct consequence of the constraining cyclization. A more detailed 2D NMR study of the native forms of fraction I and II showed the presence of multiple glycine resonances. Since the peptide contains only a single glycine, this demonstrated that there must exist more conformations (> 3) that inter-convert very slowly on the NMR timescale. These NMR results were unexpected, and almost counter-intuitive when one thinks about peptide conformations. One usually imagines peptides to be 'floppy' structures. The NMR data suggested that the disulphide-bonded retro-inverso mPGPtide presents a wide range of conformations, but that individual molecules are effectively locked into a given conformation. Based on the observed batch-to-batch variations, it would appear that our CD4 analogues randomly populate the conformational repertoire. This implies that we have little control over which populations dominate and, therefore, have little control over which batches will be biologically active.

Because the problem of batch-to-batch variations created a virtual 'dead-end' for the designed retro-inverso peptide, a structure–activity relationship (SAR) study was performed to identify the critical residues responsible for the biological activity. In this way, the information gleaned from the SAR study could be used to construct a different type of CD4 mimetic. The project was initiated by exploring the human equivalent of the murine analogue to provide species specificity comparison data. The sequence of the human and murine CDR3-like domains are shown below:

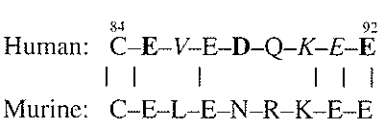

The human peptide was synthesized and an alanine scan was performed (Friedman *et al.*, 1996). For this study, a series of peptides were synthesized with a single alanine substituted for each sequence position in the parent peptide. The amino acids in the human sequence shown in bold above, indicate the residues that were shown to be

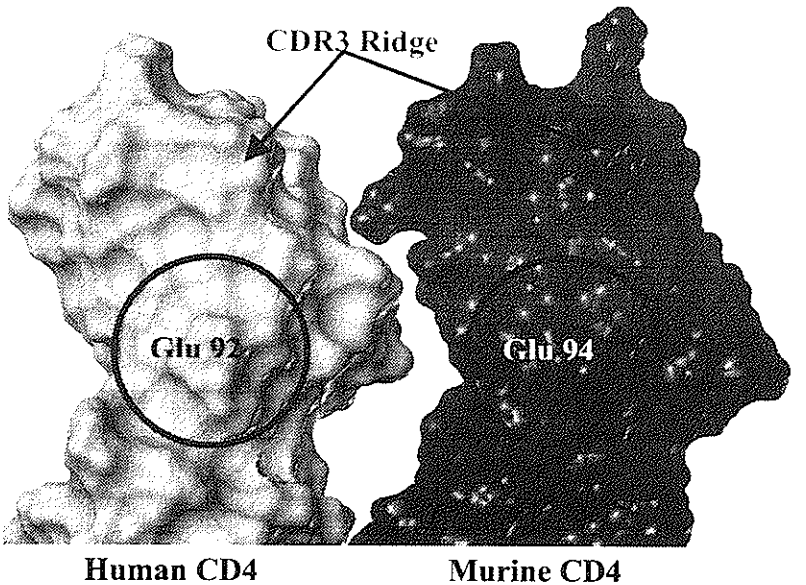

Figure 9.4. Human CD4/murine CD4 showing the active surface as determined through alanine scanning. Connolly surface representation shown here was calculated for both proteins using a theoretical sphere of 2.4 Å. Human protein is shown on the left panel (light colour) and mouse CD4 is shown on the right (dark colour). The surface areas formed by the critical glutamic acid residues in both proteins are circled. The arrows indicate CRD3-like regions.

critical for the observed biological activity (the amino acid sequences shown in italics represent amino acids that could be substituted without any observed effect). The CDR3s from the human and murine CD4s have qualitative differences in their surface presentation (see *Figure 9.4*). We examined the surface comparison in order to determine whether or not any of the biologically critical residues identified through the alanine scan were conserved between the human and murine proteins. The surface presented by the carboxy terminal glutamic acid (residue 92 in the human sequence and residue 94 in the murine sequence) had similar surface presentations on the human and mouse proteins. Consequently, we designed analogues based on this core observation.

A pharmacophore is the smallest unit that retains reproducible, biological activity. We designed a series of analogues based on the side chain presentation of the glutamic acid, searching for the pharmacophore. The structure and activity of the core analogue (ER_1) and several of the related compounds are shown in *Figure 9.5*. If the region of the ER_1 analogue corresponding to the carboxylic acid moiety of the glutamic acid side chain was modified to an amide group, the analogue completely lost its inhibitory activity. There have not been any batch-to-batch variations observed with these compounds and the analogues are highly amenable to improvement. The basic unit has an amide group at one end, followed by a glutamic acid side chain, a nitrogen, a carbonyl and a methyl group. Modification of any of these elements results in a loss of activity (data not shown). The activity appears to be modulated by addition to the terminal methyl group (*Figure 9.5*).

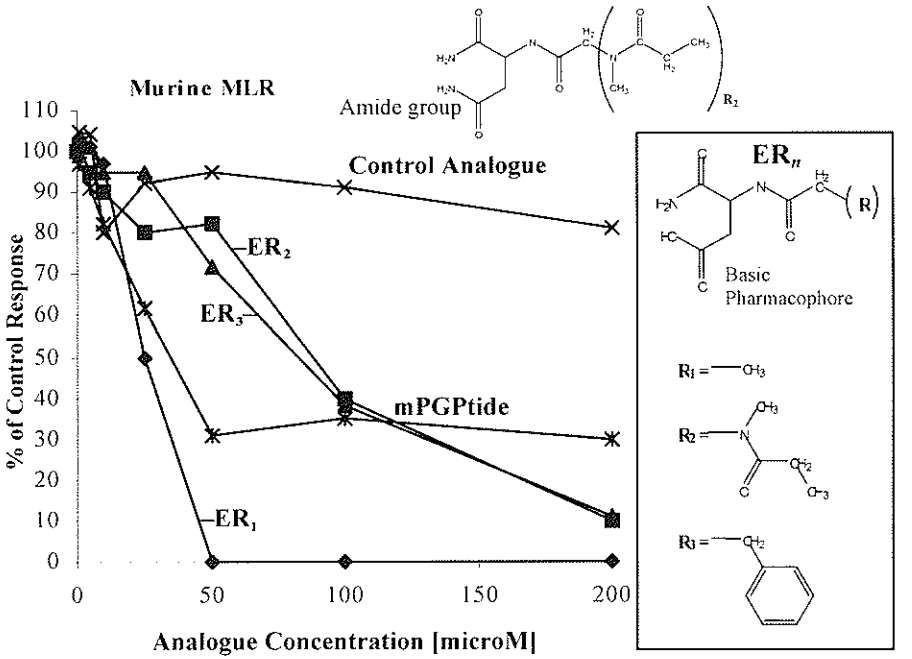

Figure 9.5. Titration of the glutamate-based CD4 mimetics in a murine MLR. The MLR was done as previously described (Jameson *et al.*, 1994). Concentrations of 200, 100, 50, 25 and 0 micromolar were used in this study. The compounds used to generate each of the individual activity profiles are indicated on the figure. The ER_n analogues were synthesized according to standard Fmoc procedures. The structures of the control and experimental compounds are shown above. The mPGP activity profile has been added for comparison.

The addition of the R_1 group ($-CH_3$) to the pharmacore creates a compound that inhibits both the murine and human CD4-dependent MLRs (as expected from the protein surface analysis). The two R groups, R_2 and R_3, were incorporated to mimic the murine surface (for selectivity). These are bulky attachments that give rise to analogues with slightly better activity than the original analogue, mPGPtide (*Figure 9.5*). These analogues, however, have a molecular weight about 5 times smaller than the original parent analogue and possess highly consistent biological activities. The use of a single methyl group attachment (R_1) gave us the best activity observed to date (the specificity of this compound still needs to be verified).

As an initial *in vivo* test of this compound series, we induced an antiviral response in mice. This model was used as a preliminary means of validating the *in vivo* activity of the ER_3 compound (this derivative showed specificity toward the murine system, data not shown). The model employed the use of C57/BL mice to generate a well-characterized CD4-dependent response to a murine retrovirus, MuLV (Panoutsakopoulou *et al.*, 1998). In this system, the CD4-dependent response is used to drive the cytotoxic T lymphocyte (CTL) response. A single bolus injection of the active analogue (ER_3) was administered *i.v.* after the helper T cell response had been initially generated, and then once more after a re-challenge with the MuLV. After three weeks, the animals were sacrificed and the CTLs were assayed for their ability to recognize

the MuLV-env protein (target-specific killing response) and for their ability to respond to novel stimuli (an allogeneic stimulation). The data derived from this study is shown in *Figure 9.6*. As one can see from the presented data, the non-specific killing response of the naïve animals was relatively high (between 5–10% target lysis). The bolus administration of the ER_3 analogue brought the antiviral response down to background levels, consistent with the notion that it induced a functional deletion of the activated CD4+ T cells. In terms of response to the *de novo* stimulus, 2 of the 8 mice injected with the ER_3 analogue had slightly diminished responses. Further studies will show whether or not this is a potential concern for the activity profile of the analogue.

In summary, it appears likely that the 3 CDR-like domains of CD4 are involved in the direct contact of the MHC class II (in analogy to the observed contacts of CD8 with MHC class I, see the section below for details). All of the structure/function studies conducted to date indicate that a protein involved in delivering a part of the primary activation signal for helper T cells binds to the externally exposed side of the CDR3-like domain of CD4 as it descends toward the cell membrane. Our efforts to design a peptide-based 'lead' were thwarted by our inability to control the conformational repertoire of the designed peptide. A systematic SAR study of an active CDR3-derived peptide has led to the development of an organic-based mimetic. Time and future studies will show the potential promise of these analogues.

Targetting the CD8 protein–protein interactions on cytotoxic T cells

In the design of our CD4-based analogues described in the preceding section, we described a structure/function hypothesis that was used to identify a local surface template on the protein upon which a rational drug design project could be built. The hypothesis was centred on the notion of functional analogy. Knowing that the CDR domains of an antibody, a structurally related family member of CD4, are involved in mediating high specificity, functionally important interactions, we hypothesized, through analogy, that the CDR-like domain of the CD4 would be important for its functional activity. In this section, we describe the use of the CD8 protein as a protein template for designing surface mimetics. In this series of studies, we have used a general structure-based hypothesis to identify a local surface area that could serve as a *de novo* drug design template.

The goal of this study was to design analogues that could potentially be used to treat pathologic conditions related to an activated CD8-dependent cytotoxic T cell response. Similar to the therapeutic strategy employed in the design of the CD4-based analogues, we wanted to test the idea that disruption of the primary T cell activation signal can be used as a means of selectively deleting only the activated subset of T cells involved in an immune response. In this case, however, instead of targetting the CD4-dependent helper T cells, we targetted the CD8+ cytotoxic T lymphocytes (CTLs). By creating an appropriate mimetic of the CD8 surface, we wanted to induce functional anergy or apoptosis, via signal disruption, that could be exploited to create a 'hole' in the immunological repertoire. The ultimate aim of the study was to enable the development of new therapeutic strategies to treat selected forms of autoimmunity, such as type I diabetes, and to treat the rejection symptoms that accompany transplantation procedures.

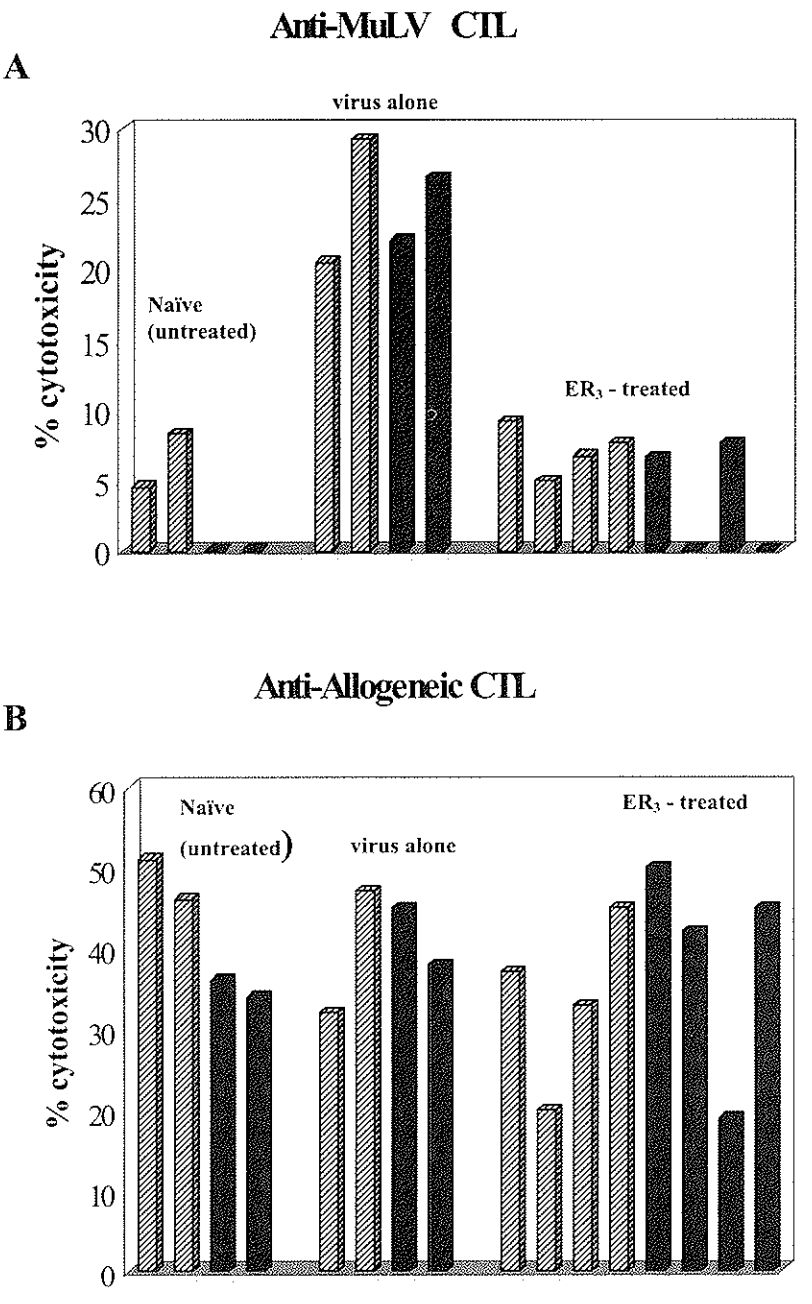

Figure 9.6. Effects of the ER_3 analogue in an *in vivo* anti-MuLV response assay. C57BL/J6 mice were used in this experiment. Treatment groups are indicated above the grouped bars. Each bar represents the data derived from an individual animal. The animals from the first study are the grey bars and the animals from the second are the black bars. Each sample was assayed at 100:1, 50:1, 25:1 responder–to–target ratios. Data shown are at 50:1 ratio. Panel A: MuLV-specific activity. Syngeneic targets kill 5–10%. Panel B: Allogeneic response to the novel stimuli.

The CTL response involves an initial clonal expansion process that results in a set of activated CD8+ T cells, similar to that which occurs with respect to CD4+ T cells. This activated set of cells is responsible for creating the effector cell population that targets and kills cells that do not bear the 'self' MHC I or harbour a foreign antigen in the context of its 'self' MHC I. These proliferating cells are highly sensitive to the fidelity of the activating signals. The sudden loss of one or more of the critical signals generally results in the induction of either apoptosis or anergy (Janeway, 1992). T cells are particularly sensitive to the regulatory signals that drive the cell cycle forward. Thus, given our understanding of the CTL activation process, it should be possible to design a small molecule that disrupts the T cell activation cluster (without affecting the resting cells that do not exhibit this protein clustering) as a means of functionally deleting the activated set of T cells.

CD8 was selected as a target because it is expressed on a limited subset of T cells and is a phenotypic marker for this class of CTL. As opposed to the polymorphic T cell antigen receptor or MHC, the sequence of CD8 is conserved across a given species. Moreover, we had access to high resolution crystal structures of both the murine (Kern *et al.*, 1998) and human (Leahy *et al.*, 1992; Gao *et al.*, 1997) proteins. Furthermore, within these structure sets, we had examples of the free protein as well as in complex with MHC class I. Most importantly, CD8 is directly involved in the generation of the primary activation signal. On a resting T cell, CD8 is unencumbered, i.e. it is not complexed with any other proteins. Upon activation, CD8 becomes a part of a multi-protein complex that aids in creating the activation signal. Therefore, it seemed reasonable to assume that a region of the solvent-exposed surface of the CD8 alpha-chain was directly involved in specifying a protein–protein contact that would be critical to the proper functioning of the T cell activation cluster.

The task of selecting a specific surface site to serve as a design template was complicated by the fact that there was no existing body of information indicating where other proteins in the T cell activation cluster bound to CD8. We based our site selection on the hypothesis that globular proteins tend to have generic surface features (both mechanical and chemical) used to specify potential protein contact points.

A survey of known protein–protein interactions, such as RAS/SOS (accession code 1BKD [Boriack-Sjodin *et al.*, 1998]), growth hormone/receptor (accession code 3HHR [De Vos *et al.*, 1992]), tumour necrosis factor/receptor (accession code 1TNR [Banner *et al.*, 1993]), CD4/gp120 (accession code 1GC1 [Kwong *et al.*, 1998]), RhoA/rhoGAP (accession code 1TX4 [Rittinger *et al.*, 1997]), and MHC class I/CD8 (accession code 1AKJ [Gao *et al.*, 1997] and 1BQH [Kern *et al.*, 1998]), reveals that the surface sites used to recognize a protein-binding partner have well defined topologies. The surfaces invariably consist of a series of ridges and surface channels. Although the generic rules describing the surface-critical features driving two proteins to specifically interact with one another are poorly understood, it is clear that a simple geometric fitting of the Van der Waals surfaces cannot completely account for the observed specificity. The alignment, ordering and dispersal of solvent-associated molecules are intimately involved in the interaction process (Cheng and Rossky, 1998; Pardanani *et al.*, 1998), as is a 'mechanical' fitting or optimization of the interacting surfaces. One would assume that a potential interaction site would possess some elements of mechanical flexibility.

The CD8 protein, a member of the immunoglobulin superfamily of proteins, has

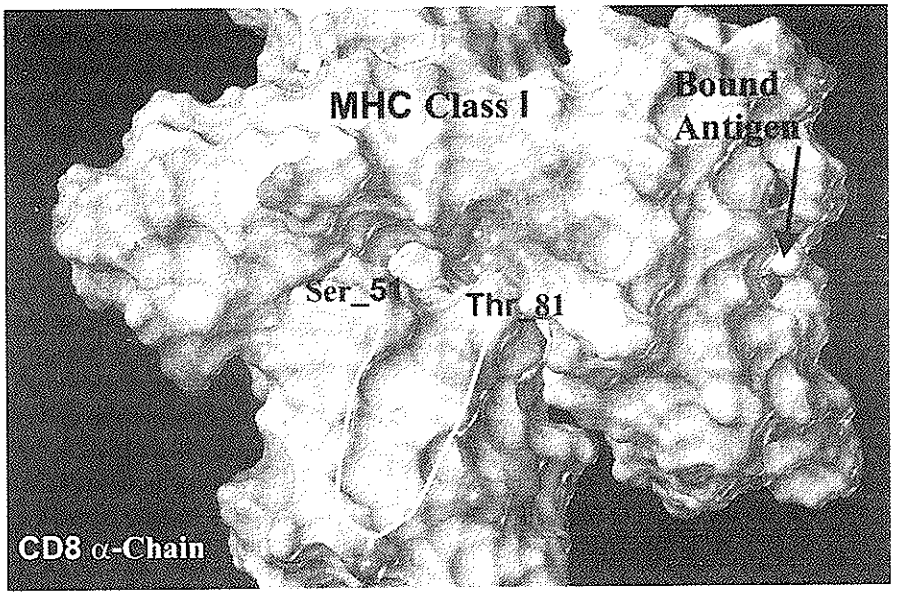

Figure 9.7. Crystallographic structure of the CD8 α-chain complexed with the MHC Class I. The structure shown above represents a Connolly surface [calculated with a theoretical sphere of 2.4 Å]. The white line drawn on this figure shows the backbone positioning of amino acids 59 to 81 and constitutes the area selected for our analogue design studies.

three surface exposed loops analogous to the complementarity-determining regions (CDRs) of an antibody. The CDR-like regions of the unbound human CD8 form ridges (with a high electropotential) that flank a channel running between the CDR3/CDR1 and CDR2. The ridges formed by the CDRs are associated with a high degree of atomic motion, relative to the rest of the protein (Leahy *et al.*, 1992). This well defined topographical surface is used to bind the MHC class I complex (Gao *et al.*, 1997).

The bound complex of the murine CD8 α-chain/MHC I is shown above in *Figure 9.7.* Inspection of the surface indicates that there is a 'ridged channel' that runs from Ser59 through Thr81. In accordance with the simplified criteria outlined above, this site was selected as a template for the analogue design studies.

In addition to the topological criteria, our laboratory has been seeking other 'mechanical' factors that can be used to localize sub-sites within the surface that can be used as specific design templates. Empirically, we have observed that analogues designed from a region that protrudes into the solvent, but has a relative degree of rigidity, tend to have the best biological activities. Entropic considerations suggest that the degree of flexibility of a given protein region should be proportional to its solvent exposure. *Figure 9.8* shows a plot of the fractional surface exposure of the amino acids 59–87 overlaid with a plot of the factors describing the atomic mobilities (known as B factors, derived from the crystallographic measurements) for the same amino acids. As can be seen in the figure, the solvent exposure parameters parallel the mobility factors for most of this region. The region between Met78 and Lys84 represents an exception to this trend (notably Arg79, Asp80 and Thr81). This region is solvent exposed; yet it is relatively rigid.

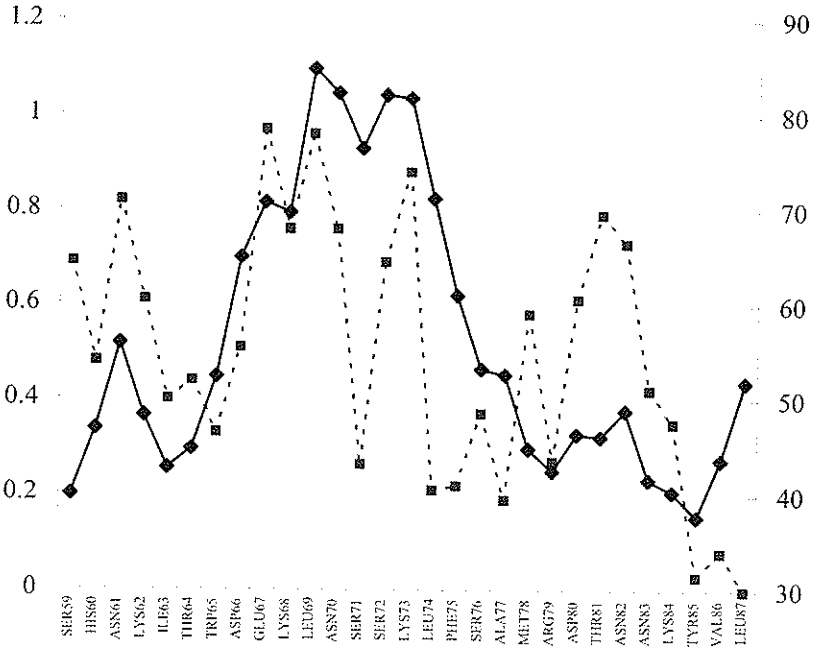

Figure 9.8. Plot of amino acid surface exposure versus B factors. The left-hand scale is the fractional solvent exposure (dotted line); the right-hand scale is the B factors taken from crystallographic study (Kern *et al.*, 1998).

As an initial attempt to map the binding-critical regions of this surface, we synthesized ~ 50 small peptide analogues derived from the exposed regions of the surface (residues 59–83). The peptides were synthesized in an overlapping fashion, incorporating three amino acids from the linear sequence with or without the addition of flanking cysteines as conformational restraints.

Our panel of α-chain-derived analogues was screened in an allogeneic CTL assay (for details, see Tretiakova *et al.*, 2000). Of the original 50 analogues tested, only four analogues exhibited dose-dependent inhibition of the CD8-dependent CTL, without having any effect on the CD4-dependent MLR (K-I-T, c-D-E-K-c, c-S-S-K-c, and c-R-D-T-c). We have focused our efforts on the best of these inhibitors, derived from the α-chain residues Arg79, Asp80 and Thr81. In the design of this analogue, computer modelling studies indicated that the unrestrained peptide did not match the R-D-T surface found in the context of the native protein (*Figure 9.9*). The cysteines-restrained analogue, on the other hand, displayed a conformational repertoire that overlapped with that of the native protein. The cRDTc analogue dose dependently inhibited the *in vitro* CTL response (Tretiakova *et al.*, 2000). As predicted by the modelling studies, the unrestrained analogue, R-D-T-N, did not have any activity, although it shared the same core amino acid sequence RDT. In the murine crystal structure, the side chains of the RDT sequence make the greatest contribution to the presentation of this local surface. To test the assumption that the observed biological activity is due to surface mimicry of the cRDTc analogue, the reverse sequence of the

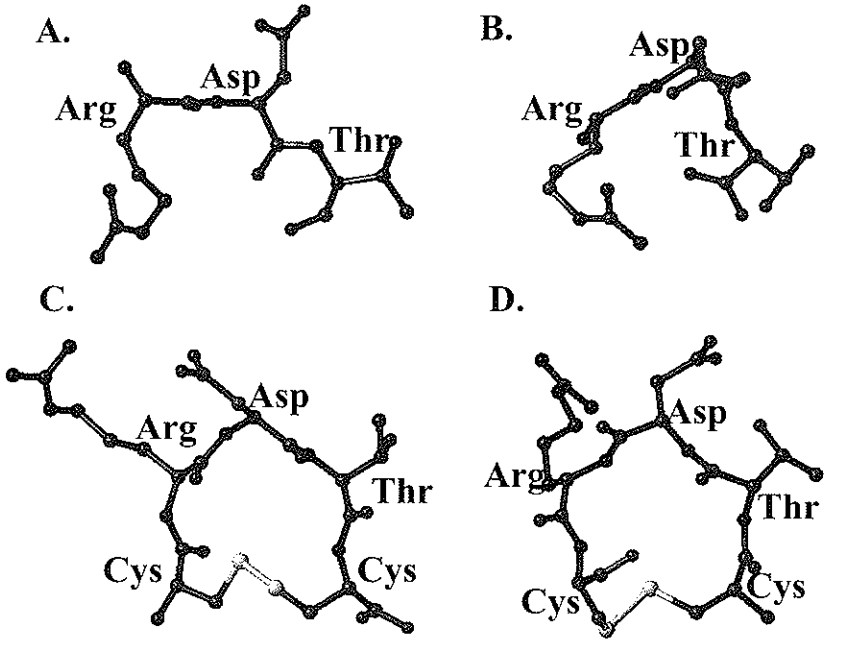

Figure 9.9. Analogue designs. Peptides were modelled on the Octane and O2 computers using Sybyl6.7 software package (Tripos and Associates, St. Louis, MO, USA). Explicit dynamics and minimizations were applied to the solvated peptides. The hydrogens, along with the water molecules, were deleted (after the computations) for the clarity of the figure. Panel A: the conformation of the RDT ridge naturally present within the CD8 protein context. Note that the side chains of Asp and Thr are in the same plane. Panels B, C, and D: models of the unrestrained RDT peptide, restrained CRDTC peptide and restrained CTDRC peptide, respectively. Note that the Asp and Thr side chain conformations in Panels D and C resemble Asp and Thr presented within the native CD8 protein (Panel A). In the unrestrained (Panel B) peptide, those critical amino acid side chains collapse upon the Arg.

analogue was also synthesized and assayed, cTDRc (*Figure 9.9*). The observation that the cTDRc has retained full biological activity indicated that the activity was primarily due to the side chain components and not the backbone nitrogens and carbonyl groups. None of the analogues had any detectable inhibitory activity in the CD4-dependent MLR. The assay data indicated that the inhibitory properties of the cRDTc analogue were both dose dependent and conformationally dependent, and that the activity derived from the amino acid side chains, rather than the backbone.

In order to characterize and develop the activity of the cRDTc analogue, we performed a structure–activity relationship (SAR) study of the analogue. On the assumption that the analogue's specificity is conferred by its side chain arrangements, the SAR was set up to characterize the individual side chain contributions to the overall activity profile. The first position to be modified was the initial arginine, while keeping the other two positions constant (note that the Arg79 is partially buried on the CD8's surface, see *Figure 9.8*). The arginine position was probed with its optical isomeric form, 'D' arginine, with a shorter chain, positively charged, lysyl replacement, and finally by truncating the position to a single hydrogen (glycine). Replacement of the arginine with its chiral enantiomer appears to have had little effect on the

activity profile of the analogue. There was a slight loss of activity (this pattern was observed across all of the assays) when the arginine was replaced with either a lysine or glycine. The analogue cDTc had no activity. We surmised that, although there may have been a small contribution from the guanidinyl group, this position most likely contributes to the appropriate overall conformation of the aspartate and threonine positions.

We also probed the relative contribution of the aspartate. For this study, we altered the chain length of the side chain (from aspartate to glutamate) and altered the functional moiety from a carboxylic acid to an amide (aspartate to asparagine and aspartate to glutamine). The pattern that emerged from repetitive assays is that the acid moiety at the end of the chains was more critical to the activity profile than was the chain length of the side chain. The cRQTc was nearly devoid of activity.

Our final SAR study sought to explore the functional contribution of the threonine. Threonine is a β-substituted amino acid with a methyl group and hydroxyl group attached to the β-carbon of the side chain. Removal of the methyl group results in the formation of serine, whereas replacement of the hydroxyl group with another methyl group results in the formation of valine. Although substitution of the threonine with either serine or valine resulted in a loss of activity, there was a relative preference for the valine substitution. The side chain of the Thr81 in the native protein appears to make a large contribution to the formation of the local surface. We therefore opted to elongate the side chain by replacement with an aromatic ring. Unexpectedly, replacement with a tyrosine resulted in a significant improvement in the activity profile of the analogue. We also tested an aromatic ring substitution without the hydroxyl moiety (cRDFc). This analogue had no activity in the CTL assay. Presumably, the aromatic ring of the tyrosine positions the hydroxyl group as a potential hydrogen bond donor.

As was the case with the CD4 analogues, we set up an *in vivo* validation assay for the cRDTc analogue. The concept inherent within the overall design process was that the analogue should inhibit the T cell activation cluster, thereby perturbing the primary activation signal and, consequently, inactivating or deleting the activated set of CTLs. If the intended mechanistic action of the analogue was as anticipated, then one would expect that an inoculation of the cRDTc, given once the activation process has been initiated, should be able to 'knock-out' an on-going CTL response in a whole animal. For this study, we used a well characterized response to an E55+ murine leukaemia virus (MuLV) infection in BALB/c mice (Avidan *et al.*, 1995; Panoutsakopoulou *et al.*, 1998). Immunocompetent BALB/c mice infected with the E55+ MuLV (a murine retrovirus) have an acute phase of viral growth, followed by a CD8-dependent clearance of the circulating virus (Avidan *et al.*, 1995). If administration of the test analogue, cRDTc, can selectively delete or inactivate the CD8-positive CTL response to the virus during the acute infectious phase of its life cycle, then it should prevent viral clearance. Four study groups were used in this assay, each consisting of 7 mice per group. The first group received virus alone without any further treatment. Consistent with previously published reports (Avidan *et al.*, 1995; Panoutsakopoulou *et al.*, 1998), all of the control mice had cleared the virus within 8 weeks (see *Table 9.2* for a data summary). The next group of mice was treated three times with an anti-CD8 mAb (clone 2.43), at 2 days before the initial viral infection, on day 0, and at 2 days post-infection. Under these conditions, the antibody inactivates the entire circulating repertoire of CD8-positive CTLs. Because of the long half-life of the antibody,

Table 9.2. Data summary of the E-55+ MuLV viral clearance assay in BALB/c mice.

Treatment group	Log_{10} viral titre	Standard deviation
Virus alone (n = 7)	0	0
Anti-CD8 mAb (n = 7)	4.03	0.82
CRDTc (n = 7)	3.44	1.83
RDTN (n=7)	0	0

The 400 micrograms of each peptide were inoculated via tail vein injection on days 10 and 17 of the study. The details of this study are described in Tretiakova *et al.* (2000).

the injected mice are unable to mount a CTL response to the virus and, consequently, are unable to clear the viral infection. A viral focus-forming assay conducted with the splenic harvests at the end of the study revealed that 100% of the antibody-treated mice had failed to clear the E55+ MuLV infection. The third group of mice was treated with 400 micrograms (*i.v.*) of the cRDTc analogue at day 10 [at the onset of the CTL activation] and once again at day 17 [during the acute phase of viral growth] after the initial viral infection. The analogue was able to prevent the CTL-mediated clearance in 6 out of 7 animals. The final group of mice received the RDTN control. These mice were treated exactly the same as those receiving the cRDTc, yet no effect on the viral clearance was observed (*Table 9.2*). A similar study was also undertaken to ask whether or not similar results could be achieved by a single dose of the analogue at half the dosage, i.e. 200 micrograms/mouse. These data are presented in *Figure 9.10*. This study also included the reverse analogue, cTDRc, which showed similar inhibition profile to the cRDTc in the *in vitro* assays. As one can see from the data shown in *Figure 9.10*, the experimental outcome was consistent with the original study (*Table 9.2*).

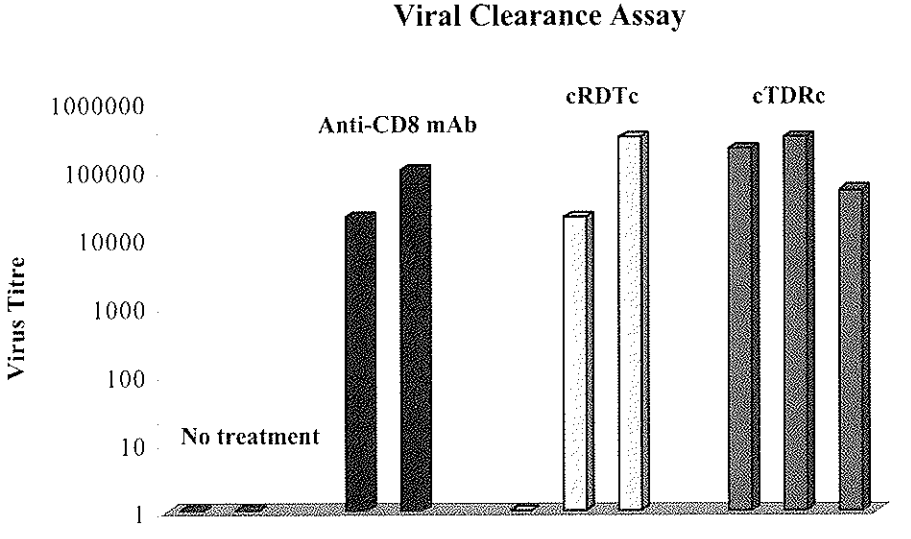

Figure 9.10. MuLV clearance assay in BALB/c mice. The treatment groups and the numbers of the animals used are indicated on the graph. The mice were treated as described previously (Tretiakova *et al.*, 2000). Briefly, the mice were injected with 1 × 105 FFU of the MuLV *i.p.* on day 0 of the experiment. The CD8 antibody treatment was as described in Panoutsakopoulou *et al.* (1998). cRDTc and cTDRc (200 microgram) were injected on day 10 of the experiment. The mice were sacrificed eight weeks after; the spleens were harvested and the viral titre was determined exactly as described in Panoutsakopoulou *et al.* (1998).

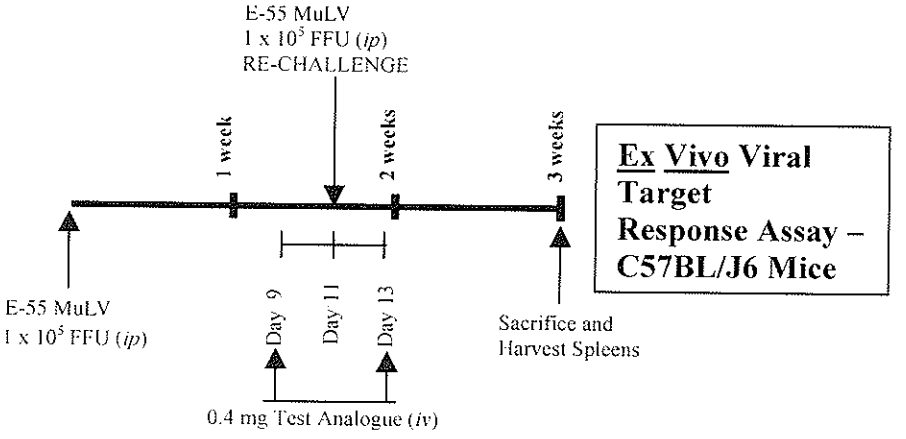

Figure 9.11. A schematic diagram of the viral target response study in C57BL/6 mice. Mice were infected *i.p.* with 1×10^5 Focus Forming Units (FFU) of the E-55$^+$ MuLV virus on experimental day 0. The immune response to the MuLV was allowed to develop, and the first dose of the analogues (200 microgram/dose) or anti-CD8 monoclonal antibody (50 microgram/dose) was administered on day 9 via the tail vein injection and *i.p.* injection, respectively. On day 11, the animals were re-challenged with a second 1×10^5 dose of the MuLV (*i.p.*). The secondary response develops much faster, therefore the second dose of the analogue or antibody was administered 2 days after re-challenge (on day 13). On day 21, the animals were sacrificed and the spleens were harvested for the *ex vivo* CTL assay.

The second *in vivo* validation model was a viral target response study in C57BL/J6 mice. A schematic time-line for this model is shown in *Figure 9.11*. The data obtained for the initial study in our second validation model, using a dosage of 400 micrograms/mouse of the analogues, is summarized in *Table 9.3*. The mice studied here were first primed *in vivo* with the MuLV, treated (or not), and their splenocytes harvested. Half of the cells were used to assay for antiviral responses and the other half were plated in an allogeneic stimulation assay, without any further treatments, to show that no generalized immunosuppression had occurred. The profile that emerged from this study clearly showed that cRDTc ablated the antiviral response generated in the mice, similar to the response observed in mice that had never received the virus; while the control analogue, RDTN, had no effect on the system. The cRDTc, however, had absolutely no effect on the ability of the splenocytes to generate a new response. Thus, the effect of the analogue was to remove the CD8+ response directed against the MuLV without impairing the function of resting lymphocytes within the animal.

In the second part of this study, we asked whether or not similar results could also be obtained using half the initial dosages. For data shown in *Figure 9.12*, the mice were divided into 6 treatment groups. The first group received no treatments (N = 4), i.e. they were naïve animals. As anticipated, this group did not specifically lyse the virus-infected targets, but were able to mount a strong allogeneic response. The second group of mice (N = 3) received the E55+ MuLV inoculation without any additional treatments. These animals were able to mount a strong anti-virus response, as well as a strong allogeneic response. The third group of mice (N = 5) received the anti-CD8 mAb at days 9 and 13 (the same treatment schedule as was given for the test analogues). These mice showed a significant reduction in their antiviral responses. Their response to the general allogeneic stimuli, however, was approximately half of

Table 9.3. E55+ MuLV target response assay in C57BL/J6 mice.

Treatment group	% Cytotoxic response	
	Antiviral response	Allogeneic response
No treatment (n = 5)	1.6%	51.4%
Virus alone (n = 5)	45.2%	50.4%
cRDTc (n = 7)	3.4%	55.2%
RDTN (n = 5)	47.8%	38.4%

The 400 micrograms of each peptide were inoculated via tail vein injection on days 9 and 13 of the study. The details of this study are described in Tretiakova *et al.* (2000).

the response seen in the other treatment groups. The fourth group of mice (N = 3) received the control analogue, RDTN. This treatment group showed a response pattern similar to that of the mice that were treated with virus alone. The fifth group of mice (N = 4) received the cTDRc analogue. This group of mice was unable to mount a significant anti-virus response, yet maintained a robust allogeneic response. Finally, the last study group (N = 4) was treated with the cRDTc analogue. These mice were also unable to mount a response against the viral targets, indicating that the activated CD8+ CTLs were absent, but mounted a robust response to the allogeneic stimuli. Taken together, these data are consistent with the previous study, as well as our experimental hypotheses.

The last set of data was designed to examine whether the inhibition of cytotoxicity that we observed in the above experiments was due to quantitative or qualitative changes induced by our experimental analogue in the antigen-specific CD8+ T cell population. For this purpose, we employed the newly developed tetramer technology that allows us to both quantitate and phenotype antigen-specific CD8+ T cells in a mouse model of influenza type A infection. In this set of data, we show the effects of our experimental analogues [we used the cRDYc analogue instead of the cRDTc analogue because it has as better potency and, consequently, exerts its activity in a single bolus injection] on CD8+ T cells that are directed against the influenza virus type A nuclear protein $NP_{(324-332)}$ immunodominant epitope. For this experiment, a CD8+ CTL response was generated against influenza in C57BL/J6 mice by immunizing mice with influenza virus type A. Pulmonary virus-specific CD8+ T cells were visualized on a flow cytometer (FACS Calibur®, Becton-Dickinson), using the NPP tetrameric complex (described in the legend of *Figure 9.13*) for staining the cells that recognized the immunodominant epitope of the nucleoprotein of influenza. Three groups of six mice each were used in this pilot study. The first group of mice was infected with influenza without any further treatments; the second group of mice was treated as the first group, except that they received a single bolus injection of the cRDYc analogue on day 7 of the study; while the last group of mice was treated on day 7 with a control peptide, cKQFc. Representative data from this study are shown below in *Figure 9.13*. There were no differences observed between the untreated controls and the group treated with the control peptide (data not shown). In the figure, one can clearly see that the activated set of NPP-specific cells is dramatically reduced in the cRDYc-treated animal (shown in the overlap between the two boxes in the lower right-hand panel of *Figure 9.13*). The averaged data from the six mice treated with the active analogue and the untreated group are shown in *Figure 9.14*. From our analysis

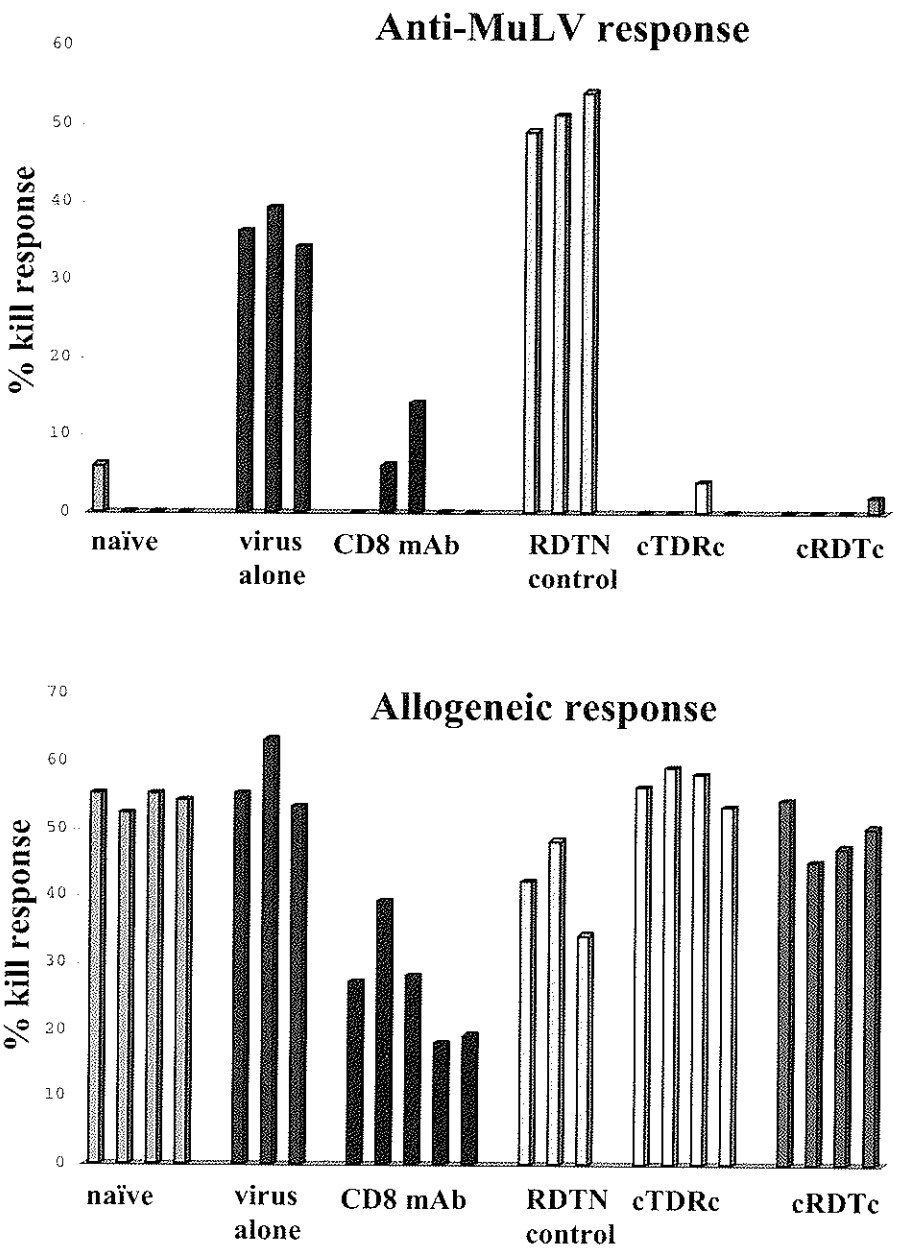

Figure 9.12. Effects of the RDT-based analogues and the CD8 antibody in the viral target response study. The treatment groups are indicated below the grouped bars. The samples were assayed at 100:1, 50:1, 25:1 responders–to–targets ratio. Each bar represents an individual animal. Top panel shows the MuLV-specific response of the treated and control animals, data in the figure are at 100:1 ratio. Bottom panel shows the ability of the treated animals to respond to the novel stimuli, data shown are at 50:1 ratio. Note that the ability of the antibody-treated animals to react to the new stimuli is considerably diminished, indicating an immune suppression. In contrast to the antibody, cRTDc- and cTDRc-treated animals were able to generate full *de novo* immune response.

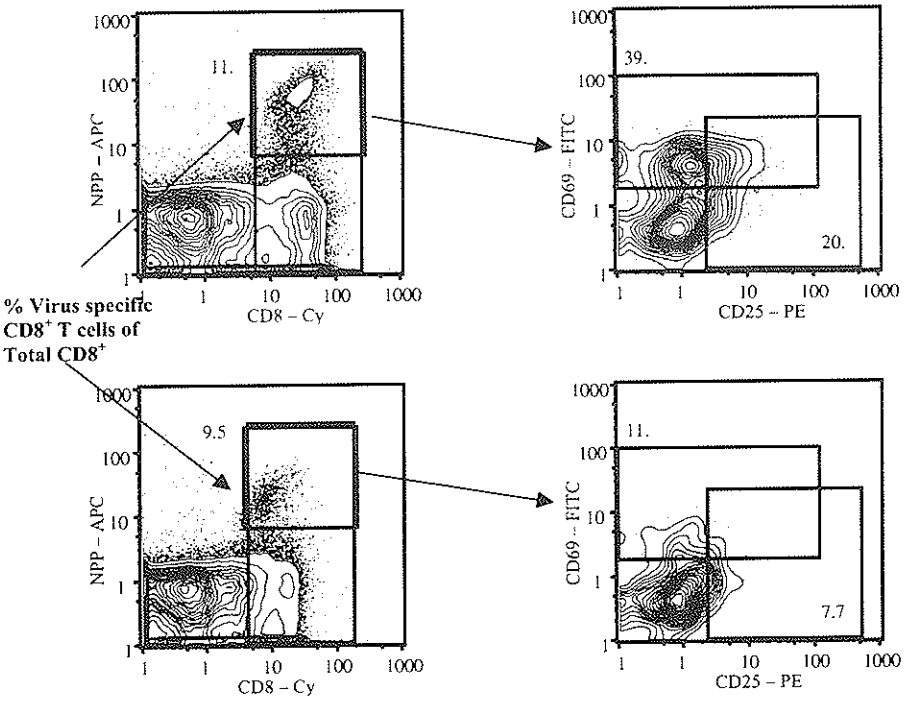

Figure 9.13. The effects of the cRDYc analogue on pulmonary influenza-specific CD8+ T cells versus untreated control. The top two panels are the flow cytometric staining patterns of a mouse, which received the virus without any further treatment. The boxed area in the upper left-hand panel shows the CD8+ population that co-stained with the NPP, representing the virus-specific cell population. The upper-hand panel is gated on the NPP-specific CD8+ cell population and shows the expression of activation markers, CD25 and CD69 on this population. The two lower panels are the cell staining patterns from a mouse treated on day 7 with the cRDYc analogue. The frequency of each population is shown in the number in the panels. The experimental procedures are described in the legend to *Figure 9.14.*

(N = 6), it is unclear whether there is an increase in the frequency of viral-specific CD8+ T cells in response to the analogue treatment (the data indicate that there is not a statistical difference; however, some of the animals had a clear increase in the overall number of CD8+ responding cells). The number of IL-2 receptor bearing cells (CD25+) is significantly reduced relative to the untreated controls. Although the data presented above are derived from pilot studies (the data need to be expanded), these data clearly show that the cRDYc-treated animals have significantly reduced influenza-specific, activated CTLs relative to untreated controls. The fact that the frequency of virus-specific CD8+ T cells is not reduced by our analogue treatment, but the expression of the IL-2R α-chain (CD25) is greatly reduced, is more consistent with the idea that we are inducing anergy, as opposed to apoptosis, and raises the question of whether, if it is anergy, the anergy is long-term.

The study presented above, in contrast to the CD4 project, is an illustration of a *de*

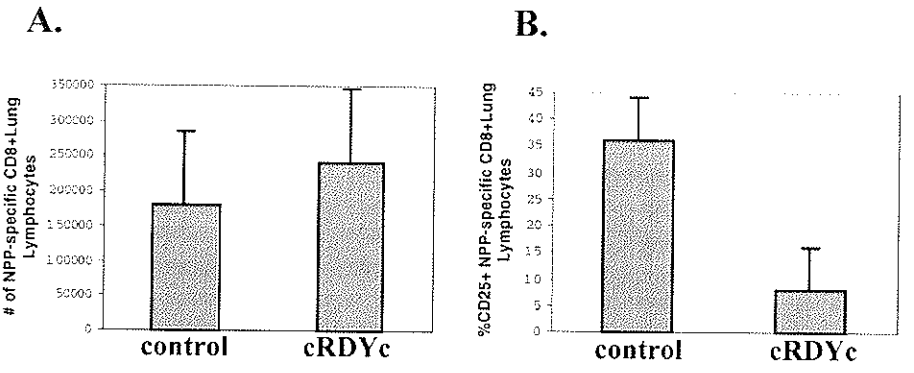

Figure 9.14. The effects of analogue treatment on influenza-specific CD8+ T cells. The data are pooled data from the cRDYc-treated mice (n = 6) and the untreated controls (n = 6). The overall cell numbers of the double-staining for NPP+ and CD8+ cells are shown in panel A. Of the pool of double-positive cells, the relative percentage of the CD25+ cells is shown in panel B. Influenza virus used in this experiment was Influenza A-Puerto Rico/8/34 (PR8, a kind gift from Dr Walter Gerhardt, University of Pennsylvania, Philadelphia, PA, USA). On day 0, C57BL/J6 mice were intranasally infected with 50 microlitres of 0.9% sterile saline containing 4 haemagglutination units (HAU) of PR8. The treated mice received a single bolus injection of 400 microgram of cRDYc or cKQFc *via* tail vein injection on day 7. The mice were sacrificed on day 10 of the assay. The analyses of the CD8+ cells were performed using the tetrameric complex staining described by Altman *et al.* (1996). Lung lymphocytes were harvested and staining was performed as described by Flynn *et al.* (1999). Cells were stained with an APC-labelled tetrameric complex of influenza nucleoprotein+H-2Db (a kind gift from Dr John Altman, Emory University, Atlanta, GA, USA) and co-stained with combinations of FITC-, Cy5PE- and PE-conjugated antibodies to cell surface markers.

novo rational design strategy. The project was initiated with a validated target, CD8. Although a crystal structure of the CD8/MHC class I complex had been solved, the surface area on the CD8 responsible for interacting with other proteins on the activated CTLs was not known. Thus, there was not a defined template for developing a rational drug design project. In the eyes of the pharmaceutical world, this represents a high-risk target. We selected our potential target site on the CD8 based on obvious topological features. *Figure 9.7* shows a Connolly surface presentation of the CD8/MHC class I complex. Upon visual inspection of the structure, one can readily see the outline of a potential protein-binding site 'footprint' that is relatively well defined. We used a semi-empirical technique with a limited number of analogues to identify the local region within this site that could be used as a specific design template. The use of the small peptides to define a pharmacophore provides a means of identifying a drug design template. The work presented above shows that the observed biological activity profiles of the lead peptides are consistent with our initial design strategies. The next steps for this study are to use the cRDTc and cRDYc as design templates for engineering organically-based analogues.

Conclusions

There are remarkably few effective drugs or treatment strategies for handling autoimmune diseases or for safely coping with the complications that arise from solid organ transplantation. In an attempt to improve the therapeutic treatment regimens,

new experimental therapies are being developed and tested. Biological applications to block the CD40/CD154 co-stimulatory pathway have shown, perhaps, the most promising activities of all of the experimental systems that have been evaluated to date (Diehl *et al.*, 2000). A non-depleting anti-CD154 antibody has been used to prolong graft survival of a full MHC mismatch in rhesus monkeys (Kenyon *et al.*, 1999; Kirk *et al.*, 1999). The antibody treatment apparently exploits activation-induced cell death (AICD) as an important feature of its therapeutic effect on prolonging allograft survival (Markees *et al.*, 1998). Additionally, it has been shown that the tolerance induced with anti-CD154 antibodies involves not only the deletion of potentially aggressive T cells, but also inhibits new cohorts of graft-reactive T cells (Graca *et al.*, 2000). Most of the studies with the anti-CD154 antibody, however, indicate that the allografts eventually reject due to arteriosclerosis. The transplant arteriosclerosis that develops in the experimental animals apparently arises from an invasion of CD8+ cytotoxic T cells (Honey *et al.*, 1999). Recent data suggest that the CD8+ T cells are not effectively targetted by the CD154 blockade (Ensminger *et al.*, 2000). Even though the CD8+ CTL response may slip through the CD40 ligand blockade, the therapeutic effects of anti-CD154 monoclonal antibody administration have been nothing short of spectacular, and seem to be devoid of any major untoward side effects (Kenyon *et al.*, 1999).

Monoclonal antibodies are playing, and will continue to play, a role as a new medical treatment regimen. These antibodies account for about a quarter of all biotech drugs in development today, and approximately 30 products that are currently in use or being investigated (Breeveld, 2000). Monoclonal antibodies, however, inherently suffer from several limitations. As is true for any relatively large protein, the cost of commercial production and purification procedures for human therapeutic use is extraordinarily high, relative to the cost of manufacturing (the more traditional) small organic drugs (Hillegass *et al.*, 1999). Although the short-term side effects of monoclonals are tolerable and predictable, long-term safety remains to be elucidated. Although *in vivo* half-lives of a week or more are not uncommon, monoclonal antibodies often have problems associated with tissue penetration, such as their inability to efficiently penetrate sinovial tissues in rheumatoid arthritis (Colcher *et al.*, 1998). In short, monoclonal antibodies will provide an immediate solution to some of the unresolved medical problems, but do not represent a long-term solution. As has often been noted by the major pharmaceutical companies, the best drug is still a classical, small organic molecule.

To borrow a phrase from Prof Herman Waldmann (Sir William Dunn School of Pathology, Oxford, United Kingdom), 'The Holy Grail of transplantation research has been to induce tolerance by a short pulse of therapy.' This is in reference to the current use of chronic therapies employing drugs, such as cyclosporin A. The rationale in developing the work presented here was to devise a strategy for engineering a short pulse therapy that exploits activation-induced cell death. In other words, the goal of our design both with respect to the CD4 and CD8 projects has been to develop a robust strategy.

Our strategic approach cannot be executed without the identification of a specific design template that can be used in the engineering of a drug. In this review, we have shown two different approaches toward the identification of design templates, one on the surface of CD4 and one on the surface of CD8. Although these approaches clearly

will not provide a universal set of rules to guide drug design groups, our efforts, together with other academic and industrial efforts, will, hopefully, help to foster the general development of rational drug design projects.

Acknowledgements

We would like to acknowledge the contributions of several key collaborators, who made these studies possible. First of all, we would like to thank Robert Korngold and his co-workers for their contributions to the CD4 project and their efforts in working out murine models for GVHD and skin grafting procedures. Markus Germann provided both the NMR expertise and analysis of our peptide-based CD4 analogues. For the CD8 project, we would like to acknowledge the efforts of Scott Little, Ken Blank, Scott Halstead, and Peter Katisikis. We would also like to thank Jack Daniels and Jim Beam for providing warmth and encouragement during the tough times.

References

ALTMAN, J.D., MOSS, P.A., GOULDER, P.J., BAROUCH, D.H., MCHEYZER-WILLIAMS, M.G., BELL, J.I., MCMICHAEL, A.J. AND DAVIS, M.M. (1996). Phenotypic analysis of antigen-specific T lymphocytes. *Science* **274**, 94–96.

AVIDAN, N., TUMAS-BRUNDAGE, K.M., SIECK, T.G., PRYSTOWSKY, M.B. AND BLANK, K.J. (1995). Effect of non-H-2-linked genes on anti-virus immune responses and long-term survival in mice persistently infected with E-55+ murine leukemia virus. *Virology* **211**, 507–513.

BANNER, D., D'ARCY, A., JANES, W., GENTZ, R., SCHOENFELD, H., BROGER, C., LOETSCHER, H. AND LESSLAUER, W. (1993). Crystal structure of the soluble human 55 kd TNF receptor-human TNF beta complex: implications for TNF receptor activation. *Cell* **73**, 431–445.

BORIACK-SJODIN, P., MARGARIT, S., BAR-SAGI, D. AND KURIYAN, J. (1998). The structural basis of the activation of Tas by Sos. *Nature* **394**, 337–343.

BREEVELD, F. (2000). Therapeutic monoclonal antibodies. *Lancet* **355**, 735–740.

BROWN, E.J. AND GOODWIN, J.L. (1988). Fibronectin receptors of phagocytes. Characterization of the Arg-Gly-Asp binding proteins of human monocytes and polymorphonuclear leukocytes. *Journal of Experimental Medicine* **167**, 777–793.

BROWN, J.H., JARDETZKY, T.S., GORGA, J.C., STERN, L.J., URBAN, R.G., STROMINGER, J.L. AND WILEY, D.C. (1993). Three-dimensional structure of the human class II histo-compatibility antigen HLA-DR1. *Nature* **364**, 33–39.

CARTEAUX, J.P., ROUX, S., KUHN, H., TSCHOPP, T., COLOMBO, V. AND HADVARY, P. (1993). Ro 44-9883, a new nonpeptide glycoprotein IIb/IIIa antagonist, prevents platelet loss during experimental cardiopulmonary bypass. *Journal of Thoracic Cardiovascular Surgery* **106**, 834–841.

CHENG, Y.K. AND ROSSKY, P.J. (1998). Surface topography dependence of biomolecular hydrophobic hydration. *Nature* **392**, 696–699.

CHOREV, M., SHAVITZ, R., GOODMAN, M., MINICK, S. AND GUILLEMIN, R. (1979). Partially modified retro-inverso-enkephalinamides: topochemical long-acting analogs *in vitro* and *in vivo*. *Science* **204**, 1210–1212.

COLCHER, D., PAVLINKOVA, G., BERESFORD, G., BOOTH, B., CHOUDHURY, A. AND BATRA, S. (1998). Pharmacokinetics and diodistrivution of genetically-engineered antibodies. *Quarterly Journal of Nuclear Medicine* **42**, 225–241.

CRAIG, J.C., DUNCAN, I.B., HOCKLEY, D., GRIEF, C., ROBERTS, N.A. AND MILLS, J.S. (1991). Antiviral properties of Ro 31-8959, an inhibitor of human immunodeficiency virus (HIV) proteinase. *Antiviral Research* **16**, 295–305.

DEGRADO, W.F. (1988). Design of peptides and proteins. *Advances in Protein Chemistry* **39**, 51–124.

DESOLMS, S.J., GIULIANI, E.A., GUARE, J.P., VACCA, J.P., SANDERS, W.M., GRAHAM, S.L., WIGGINS, J.M., DARKE, P.L., SIGAL, I.S. AND ZUGAY, J.A. (1991). Design and synthesis of HIV protease inhibitors. Variations of the carboxy terminus of the HIV protease inhibitor L-682,679. *Journal of Medicinal Chemistry* **34**, 2852–2857.

DE VOS, A., ULTSCH, M. AND KOSSIAKOFF, A. (1992). Human growth hormone and extracellular domain of its receptor: crystal structure of the complex. *Science* **255**, 306–312.

DIEHL, L., DEN BOER, A., VAN DER VOORT, E., MELIEF, C., OFFRINGA, R. AND TOES, R. (2000). The role of CD40 in peripheral T cell tolerance and immunity. *Journal of Molecular Medicine* **78**, 363–371.

ENSMINGER, S., WITZKE, O., SPRIEWALD, B., MORRISON, K., MORRIS, P., ROSE, M. AND WOOD, K. (2000). CD8+ T cells contribute to the development of transplant arteriosclerosis despite CD154 blockade. *Transplantation* **69**, 2609–2612.

ERICKSON, J., NEIDHART, D.J., VANDRIE, J., KEMPF, D.J., WANG, X.C., NORBECK, D.W., PLATTNER, J.J., RITTENHOUSE, J.W., TURON, M. AND WIDEBURG, N. (1990). Design, activity, and 2.8 A crystal structure of a C2 symmetric inhibitor complexed to HIV-1 protease. *Science* **249**, 527–533.

FLYNN, K.J., RIBERDY, J.M., CHRISTENSEN, J.P., ALTMAN, J.D. AND DOHERTY, P.C. (1999). *In vivo* proliferation of naive and memory influenza-specific CD8(+) T cells. *National Academy of Sciences of the United States of America. Proceedings* **96**, 8597–8602.

FRIEDMAN, T.M., REDDY, A.P., WASSELL, R., JAMESON, B.A. AND KORNGOLD, R. (1996). Identification of a human CD4-CDR3-like surface involved in CD4+ T cell function. *Journal of Biological Chemistry* **271**, 22635–22640.

GAO, G.F., TORMO, J., GERTH, U.C., WYER, J.R., MCMICHAEL, A.J., STUART, D.I., BELL, J.I., JONES, E.Y. AND JAKOBSEN, B.K. (1997). Crystal structure of the complex between human CD8alpha(alpha) and HLA-A2. *Nature* **387**, 630–634.

GRACA, L., HONEY, K., ADAMS, E., COBBOLD, S.P. AND WALDMANN, H. (2000). Anti-CD154 therapeutic antibodies induce infectious transplantation tolerance. *Journal of Immunology* **165**, 4783–4786.

HARTMAN, G.D., EGBERTSON, M.S., HALCZENKO, W., LASWELL, W.L., DUGGAN, M.E., SMITH, R.L., NAYLOR, A.M., MANNO, P.D., LYNCH, R.J. AND ZHANG, G. (1992). Non-peptide fibrinogen receptor antagonists. 1. Discovery and design of exosite inhibitors. *Journal of Medicinal Chemistry* **35**, 4640–4642.

HILLEGASS, W., NEWMAN, A. AND RACO, D. (1999). Economic issues in glycoprotein IIb/IIIa receptor therapy. *American Heart Journal* **138** (1 Pt 2), S24–32.

HONEY, K., COBBOLD, S. AND WALDMANN, H. (1999). CD40 ligand blockade induces CD4+ T cell tolerance and linked suppression. *Journal of Immunology* **163**, 4805–4810.

HUTCHINGS, P., PARISH, N., O'REILLY, L., DAWE, K., ROITT, I.M. AND COOKE, A. (1993). The regulation of autoimmunity through CD4+ T cells. *Autoimmunity* **15**, 21–23.

JAMESON, B.A. (1989). Modeling and peptide design. *Nature* **341**, 465–467.

JAMESON, B.A., MCDONNELL, J.M., MARINI, J.C. AND KORNGOLD, R. (1994). A rationally designed CD4 analogue inhibits experimental allergic encephalomyelitis. *Nature* **368**, 744–746.

JANEWAY, C.A. (1992). The T cell receptor as a multicomponent signalling machine: CD4/CD8 coreceptors and CD45 in T cell activation. *Annual Review of Immunology* **10**, 645–674.

KENYON, N., CHATZIPETROU, M., MASETTI, M., RANUCOLI, A., OLIVEIRA, M., WAGNER, J., KIRK, A., HARLAN, D., VURKLY, L. AND RICORDI, C. (1999). Long-term survival and function of intrahepatic islet allografts in rhesus monkeys treated with humanized anti-CD154. *National Academy of Sciences of the United States of America. Proceedings* **96**, 8132–8136.

KERN, P.S., TENG, M.K., SMOLYAR, A., LIU, J.H., LIU, J., HUSSEY, R.E., SPOERL, R., CHANG, H.C., REINHERZ, E.L. AND WANG, J.H. (1998). Structural basis of CD8 coreceptor function revealed by crystallographic analysis of a murine CD8alphaalpha ectodomain fragment in complex with H-2Kb. *Immunity* **9**, 519–530.

KIRK, A., BURKLY, L., BATTY, D., BAUMGARTNER, R., BERNING, J.K.B., FECHNER, J., GERMOND, R., KAMPEN, R., PATTERSON, N., SWANSON, S., TADAKI, D., TENHOOR, C., WHITE, L., KNECHTLE, S. AND HARLAN, D. (1999). Treatment with humanized monoclonal

antibody against CD154 prevents acute renal allograft rejection in nonhuman primates. *Nature Medicine* **5**, 686–693.

KOCH, U. AND KORNGOLD, R. (1997). A synthetic CD4-CDR3 peptide analog enhances bone marrow engraftment across major histocompatibility barriers. *Blood* **89**, 2880–2890.

KOCH, U., CHOKSI, S., MARCUCCI, L. AND KORNGOLD, R. (1998). A synthetic CD4-CDR3 peptide analog enhances skin allograft survival across a MHC class II barrier. *Journal of Immunology* **161**, 421–429.

KWONG, P., WYATT, R., ROBINSON, J., SWEET, R., SODROSKI, J. AND HENDRICKSON, W. (1998). Structure of an HIV gp120 envelope glycoprotein in complex with the CD4 receptor and a neutralizing human antibody. *Nature* **393**, 648–659.

LEAHY, D.J., AXEL, R. AND HENDRICKSON, W.A. (1992). Crystal structure of a soluble form of the human T cell co-receptor CD8 at 2.6 angstroms. *Cell* **68**, 1145–1153.

LUCCHINETTI, C., BRUCK, W. AND NOSEWORTHY, J. (2001). Multiple sclerosis: recent developments in neuropathology, pathogenesis, magnetic resonance imaging studies and treatment. *Current Opinions in Neurology* **14**, 259–269.

MARINI, J.C., JAMESON, B.A., LUBLIN, F.D. AND KORNGOLD, R. (1996). A CD4-CDR3 peptide analog inhibits both primary and secondary autoreactive CD4+ T cell responses in experimental allergic encephalomyelitis. *Journal of Immunology* **157**, 3706–3715.

MARKEES, T., PHILLIPS, N., GORDON, E., NOELLE, R., SHULTZ, L., MORDERS, J., GREINER, D. AND ROSSINI, A. (1998). Long-term survival of skin allografts induced by donor splenocytes and anti-CD154 antibody in thymectomized mice requires CD4+ T cells, interferon-gamma, and CTLA4. *Journal of Clinical Investigation* **101**, 2446–2452.

MATSUSHITA, S. (2000). Current status and future issues in the treatment of HIV-1 infection. *International Journal of Hematology* **72**, 20–27.

MCDONNELL, J.M., BLANK, K.J., RAO, P.E. AND JAMESON, B.A. (1992a). Direct involvement of the CDR3-like domain of CD4 in T helper cell activation. *Journal of Immunology* **149**, 1626–1630.

MCDONNELL, J.M., VARNUM, J.M., MAYO, K.H. AND JAMESON, B.A. (1992b). Rational design of a peptide analog of the L3T4 CDR3-like region. *Immunomethods* **1**, 33–39.

OKAMOTO, S., WATANABE, M., YAMAZAKI, M., YAJIMA, T., HAYASHI, T., ISHII, H., MUKAI, M., YAMADA, T., WATANABE, N., JAMESON, B.A. AND HIBI, T. (1999). A synthetic mimetic of CD4 is able to suppress disease in a rodent model of immune colitis. *European Journal of Immunology* **29**, 355–366.

PANOUTSAKOPOULOU, V., LITTLE, C.S., SIECK, T.G., BLANKENHORN, E.P. AND BLANK, K.J. (1998). Differences in the immune response during the acute phase of E-55+ Murine Leukemia Virus infection in progressor BALB and long term nonprogressor C57BL mice. *Journal of Immunology* **161**, 17–26.

PARDANANI, A., GAMBACURTA, A., ASCOLI, F. AND ROYER, W.E. (1998). Mutational destabilization of the critical interface water cluster in Scapharca dimeric hemoglobin: structural basis for altered allosteric activity. *Journal of Molecular Biology* **284**, 729–739.

PIERSCHBACHER, M.D. AND RUOSLAHTI, E. (1984). Cell attachment activity of fibronectin can be duplicated by small synthetic fragments of the molecule. *Nature* **309**, 30–33.

REDDY, M.R., VISWANADHAN, V.N. AND WEINSTEIN, J.N. (1991). Relative differences in the binding free energies of human immunodeficiency virus 1 protease inhibitors: a thermodynamic cycle-perturbation approach. *National Academy of Sciences of the United States of America. Proceedings* **88**, 10287–10291.

RITTINGER, K., WALKER, P., ECCLESTON, J., SMERDON, S. AND GAMBLIN, S. (1997). Structure at 1.65A of RhoA and its GTPase-activating protein in complex with a transition-state analogue. *Nature* **389**, 758–762.

ROLAK, L.A. (2001). Multiple sclerosis treatment 2001. *Neurology Clinic* **19**, 107–118.

RYU, S.E., KWONG, P.D., TRUNEH, A., PORTER, T.G., ARTHOS, J., ROSENBERG, M., DAI, X.P., XUONG, N.H., AXEL, R. AND SWEET, R.W. (1990). Crystal structure of an HIV-binding recombinant fragment of human CD4. *Nature* **348**, 419–426.

THAISRIVONGS, S., TOMASSELLI, A.G., MOON, J.B., HUI, J., MCQUADE, T.J., TURNER, S.R., STROHBACH, J.W., HOWE, W.J., TARPLEY, W.G. AND HEINRIKSON, R.L. (1991). Inhibitors of the protease from human immunodeficiency virus: design and modeling of a compound

containing a dihydroxyethylene isostere insert with high binding affinity and effective antiviral activity. *Journal of Medicinal Chemistry* **34**, 2344–2356.

TOWNSEND, R.M., BRIGGS, C., MARINI, J.C., MURPHY, G.F. AND KORNGOLD, R. (1996). Inhibitory effect of a CD4-CDR3 peptide analog on graft-versus-host disease across a major histocompatibility complex-haploidentical barrier. *Blood* **88**, 3038–3047.

TOWNSEND, R.M., GILBERT, M.J. AND KORNGOLD, R. (1998). Combination therapy with a CD4-CDR3 peptide analog and cyclosporin A to prevent graft–vs–host disease in a MHC-haploidentical bone marrow transplantation model. *Clinical Immunology and Immunopathology* **86**, 115–119.

TRETIAKOVA, A.P., LITTLE, C.S., BLANK, K.J. AND JAMESON, B.A. (2000). Rational design of cytotoxic T-cell inhibitors. *Nature Biotechnology* **18**, 984–988.

WLODAWER, A., MILLER, M., JASKOLSKI, M., SATHYANARAYANA, B.K., BALDWIN, E., WEBER, I.T., SELK, L.M., CLAWSON, L., SCHNEIDER, J. AND KENT, S.B. (1989). Conserved folding in retroviral proteases: crystal structure of a synthetic HIV-1 protease. *Science* **245**, 616–621.